Organic Process Research & Development

ARTICLE

pubs.acs.org/OPRD

Coupling Polymorphism/Solvatomorphism and Physical Stability Evaluation with Early Salt Synthesis Optimization of an Investigational Drug

Anna Shevchenko,*[,†,‡] David Din Belle,[‡] Saara Tiittanen,[‡] Arto Karjalainen,[‡] Arto Tolvanen,[‡] Veli Pekka Tanninen,[‡] Jorma Haarala,[‡] Mikko Mäkelä,[‡] Jouko Yliruusi,[†] and Inna Miroshnyk[†]

[†]Division of Pharmaceutical Technology, Faculty of Pharmacy, University of Helsinki, P.O. Box 56, Helsinki FIN-00014, Finland

[‡]Research and Development, Orion Pharma, P.O. Box 65, FI-02101 Espoo, Finland

Supporting Information

ABSTRACT: The need for effective solid-form screening approaches, especially designed for the early discovery phases, is well recognized within the pharmaceutical industry. Here we report on the early polymorphism and solvatomorphism evaluation of a new drug candidate for selective α_{2C}-adrenoceptor antagonists ORM10921·HCl. The approach we use is based on the systematic batch-to-batch characterization of the solids generated during the salt synthesis optimization. Within this study three crystalline forms, two anhydrous and one hemihydrate, were discovered and identified by X-ray powder diffraction (XRPD), differential scanning calorimery (DSC), and thermal gravimetry (TGA). Moreover, coupling the gravimetric vapor sorption analysis with a conventional XRPD enabled the relative stability of these solid-state forms at ambient conditions to be established and the most stable form, the hemihydrate, to be selected for further development. Hence, the utilized approach has proven to be an effective and fast tool for initial polymorphism and solvatomorphism tendency evaluation of drug candidates. While it is not obvious that this approach is sufficient for a comprehensive assessment of polymorphism, it demonstrates the importance of mindful solid-state characterization during crystallization process development.

1. INTRODUCTION

The crucial need for exploring solid-state properties is commonly recognized in the pharmaceutical industry.[1−3] Ideally, the in vivo efficiency, pharmacokinetics, and toxicology studies should be performed with the drug candidates that exhibit optimal solid-state properties.[4−6] As indicated by Huang and Tong,[5] the most appropriate time for finding a suitable solid form is during the lead identification (LI) and lead optimization (LO) phases of the drug discovery process. At the later stages, the developability assessment criteria for new drug candidates are applied to identify the potential challenges and even project "stoppers" of the drug development.[4,5,7] These criteria are typically set to solubility and dissolution, hygroscopicity, stability, and synthesis process scalability of the chosen solid-state form. Estimation of scalability of the synthesis process and physical stability includes evaluation of the tendency of a new chemical entity to crystallize in different crystal forms, investigation of thermodynamic relationship between polymorphs and solvates as well as relative stability of possible solid forms at ambient conditions.[5]

A key element of the strategy to reduce the time required for preclinical development is to link solid-form discovery with formulation, formulation design, and manufacturing.[1] According to Byrn et al.,[2] the most efficient way to speed up new drug development is by means of accelerating the process of 'proof-of-concept' (POC). Specifically, this acceleration can be achieved by performing the best solid-form screenings as soon as the candidate has been selected. Knowledge about the polymorphism and solvatomorphism tendency and solid-state properties of the new candidate is of great importance for screening facilitation.

The polymorphism and solvatomorphism tendency has been the subject of numerous investigations.[8−16] It is traditionally studied through crystallization from various solvents using diverse temperature profiles and concentrations, as well as by applying an additional thermal, pressure, or mechanical treatment. Due to a limited amount of substance available at the early discovery phases, most screening methodologies were adapted for using small-scale crystallization volumes and miniaturized analysis techniques.[3,7,10,18,19] As a result, in all these approaches designed for the early discovery phase, the crystallization conditions differ significantly from those used in ordinary organic synthesis processes. First, the crystallization experiments are performed in very small (microliter scale) volumes, and second, they typically do not involve any real synthesis. These small-volume approaches have a tendency to produce metastable and amorphous forms, as well as the mixtures of them.[2] As a result of which the most stable form can remain undiscovered. Consequently, there is a practical need for development cost-effective polymorphism and solvatomorphism tendency evaluation approaches directed on discovery of the stable solid form at ambient conditions.

In this context, we have chosen a rational approach for the fast initial polymorphism and solvatomorphism tendency evaluation

Received: February 1, 2011
Published: April 26, 2011

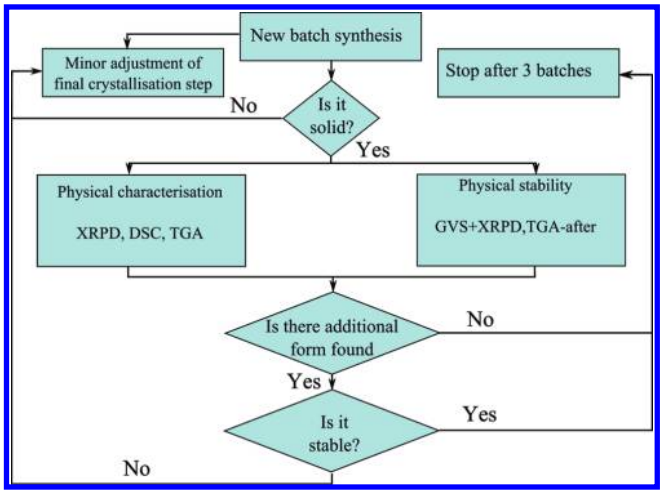

Figure 1. Flowchart for early polymorphism and solvatomorphism tendency and stability evaluation of a drug candidate.

tendency evaluation at the very beginning of the discovery process. The systematic examination of solid state properties of sequentially synthesized batches is merged with synthesis process optimization thus enabling assessment of polymorphism and solvatomorphism tendency on the real process scale. This approach is schematically presented in Figure 1. Briefly, the physical characterization of each fresh batch of a new substance is performed by means of standard methods, X-ray powder diffraction (XRPD), differential scanning calorimetry (DSC), and thermal gravimetric analysis (TGA). Simultaneously, in order to evaluate the physical stability at high relative humidity, every single batch is analyzed by the gravimetric vapor sorption (GVS) method combined with XRPD and TGA analysis performed before and after GVS. The final crystallization step of the synthesis is adjusted until a stable solid form can be reproducibly crystallized.

In this work, the approach presented in Figure 1 is applied to a new chemical entity, ORM10921 (Figure 2). ORM10921 has exhibited efficacy in rodent models predicting antipsychotic and antidepressant activity[20] and was under investigation as a new drug candidate for selective α_{2C}-adrenoceptor antagonists. This molecule is basic and shows a low water solubility (7.5 μg/mL in phosphate buffer at pH = 7.4). To enhance solubility of ORM10921 base, the salt formation approach[21,22] was employed, and a traditional hydrochloride (HCl) salt was synthesized. Hence, the focus of this study was on polymorphism and solvatomorphism tendency and stability evaluation of ORM10921·HCl, which was coupled with the early salt synthesis optimization.

2. EXPERIMENTAL SECTION

2.1. Materials. The basic drug substance candidate ORM10921 (MW = 285.38), IUPAC name [1*R**,12b*R**)-(−)-1,3,4,6,7,12b-hexahydro-1-methoxymethyl-1-methyl-2*H*-benzofuro [2,3-*a*]quinolizine], and its hydrochloric salt were synthesized by Orion Pharma, Finland. The absolute configuration was assigned by optical rotation and later by single-crystal X-ray diffraction (see Supporting Information). The optical purity of the material was >97%.

2.2. Crystallization and Off-Line Analysis. The final step of the synthesis involved the dissolving of the ORM10921 free base

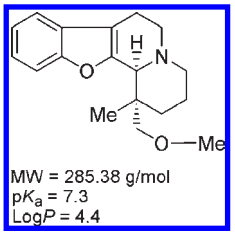

Figure 2. Chemical structure of the investigational durg, ORM10921.

in ethyl acetate or a mixture of ethyl acetate with another solvent, followed by slow addition of 10% HCl solution in ethyl acetate with a constant stirring rate. After accomplishing the salt precipitation, the slurry was cooled in an ice bath for 3 h, filtered, and washed in ethyl acetate with subsequent drying in vacuum at elevated temperature. The ethyl acetate was chosen as organic solvent because it has low toxicity and is volatile, and the free base has high solubility in the solvent (>100 mg/mL) before the counterion is added. The size of batches was 1 g. The batches were crystallized in chronological order, and the adjustments of the crystallization were made on the basis of the feedback of the results of the phase composition and stability analysis as schematically illustrated in Figure 1. The amount of material available for solid-state analysis was about 50 mg. The rest of the material was spent for other studies essential for the drug development.

2.3. Powder X-ray Diffraction (XRPD). For qualitative phase analysis the conventional X-ray powder diffraction method was used. Philips X'Pert PRO multipurpose $\theta-\theta$ diffractometer equipped with the RTMS (Real Time Multiple Strip) detector and filtered Kα radiation from Cu tube at 40 mA and 45 kV was used for the qualitative phase analysis. Due to the limited sample amount available, the powder sample was placed on a zero background sample stage that is a single crystal of silicon cut along a nondiffracting plane.

2.4. Gravimetric Vapour Sorption (GVS). The moisture sorption−desorption isotherms were measured by the humidity- and temperature-controlled microbalance system, Dynamic Vapour Sorption (DVS 1, Surface Management Systems Ltd.). The moisture sorption−desorption behavior of the samples was determined by continuous measuring of the weight change of the samples with two subsequent cycles of relative humidity (RH) each starting from 0% to 95% and backward to 0% at 10% RH steps using the equilibration condition for the mass change $dm/dt \leq 0.0003\%$ at each step. The RH generator automatically advances to the next RH step when this condition is reached. After the experiment the qualitative phase analysis was performed by XRPD in order to detect possible moisture-induced phase transformations.

2.5. Differential Scanning Calorimetry (DSC) and Thermal Gravimetry (TGA). The differential scanning calorimetry (DSC) and thermal gravimetrical analysis (TGA) were performed as supporting methods for the solid-state characterization. Melting behavior was analyzed by differential scanning calorimeter (DSC821e, Mettler Toledo AG). Accurately weighed samples of 1−3 mg were sealed in a perforated aluminum pan, and a nitrogen purge with a flowing rate of 80 mL/min was used in the furnace. The scans were performed, heating the sample from 25 to 240 °C with a heating rate of 10 °C/min.

Loss of weight was monitored with a thermobalance (TGA/SDTA 851e, Mettler Toledo AG). Samples (∼5 mg) were analyzed at a heating rate of 10 °C/min under nitrogen purge

dx.doi.org/10.1021/op200026f |*Org. Process Res. Dev.* 2011, 15, 666–672

(50 mL/min) between 25 and 300 °C. The weight loss between 36 and 180 °C was calculated.

2.6. Single-Crystal Analysis. The single-crystal X-ray diffraction data was collected using a Bruker Nonius (1998) single-crystal X-ray diffractometer. The cell refinement and data reduction were performed with DENZO and SCALEPACK software. The software to solve the structure was SHELX97 and to refine the structure SHELS97.

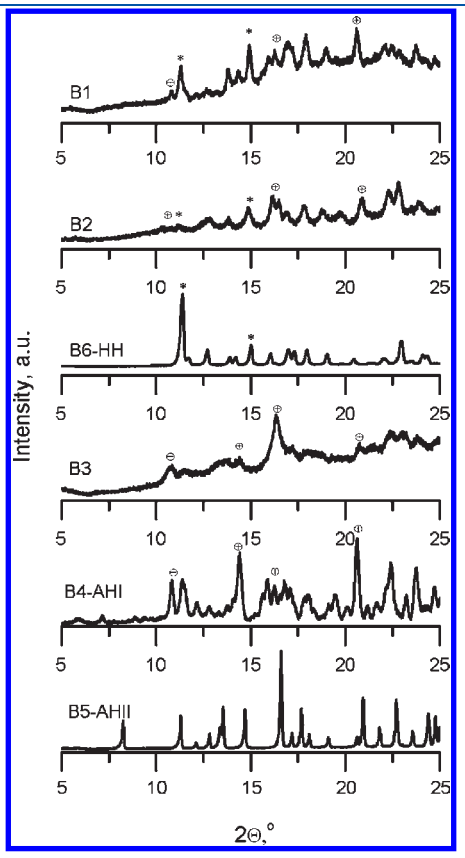

Figure 3. XRPD patterns of ORM10921·HCl batches classified on the basis of the major phase present in the sample. The characteristic peaks for HH and AHII are indicated by * and ⊕, respectively.

3. RESULTS AND DISCUSSION

3.1. Batch-to-Batch Phase Composition. Initially, qualitative phase composition analysis of the hydrochloric salt batches was performed using X-ray powder diffraction patterns displayed in Figure 3. On the basis of the XRPD results and complementary analysis of these batches by GVS and TGA, the following three crystalline solid forms of ORM10921·HCl were identified: (i) anhydrate I (AHI), (ii) anhydrate II (AHII), and (iii) hemihydrate I (HH) (Table 1). The properties of the discovered solid-state forms are described in section 3.3. Moreover, as seen in Table 1, an amorphous form (AM) was found in a number of the studied batches in variable amounts. However, none of these batches was completely XRPD-amorphous.

3.2. Moisture-Induced Crystallization of Batches Containing Amorphous Phase. According to XRPD results (Figure 3), an amorphous form was found to be the predominant solid phase for the initial three batches (B1, B2, and B3) (Table 1). The very first batch, B1, demonstrated physical instability upon exposure to conditions of high relative humidity, as revealed by GVS analysis (Figure 4A). During the first cycle, the moisture sorption curve yielded a rapid mass decrease at 55% RH, behaviour typical for amorphous material that undergoes moisture-induced crystallization.[23−25] In such cases, the sudden weight drop is associated with the expulsion of excess water by the material after crystallization.[23] In contrast, throughout the second sorption run, the mass of the sample monotonically increases as a function of RH, indicating a complete phase transformation to a more stable crystalline form. The fact of a solid-phase transition (crystallization) was further verified by XRPD (Figure 4B).

The TGA analysis of the sample after GVS showed the weight loss of 2.8% (Table 1), which is most likely due to loss of water of crystallization. This weight loss approximately corresponds to a half of water molecule per molecule of ORM10921·HCl. Summarizing the results obtained, it was concluded that upon exposure to moisture the amorphous material tends to crystallize into a more stable crystalline form, a hemihydrate (ORM10921·HCl·1/2 H2O; hereafter denoted as HH).

The following two batches, B2 and B3, were produced by varying drying temperature. The only change caused by lower drying temperature of the batch B2 was significantly increased TGA weight loss from 1.8 to 7.6%. With an elevated drying temperature applied for the batch B3, a double effect was

Table 1. Results of batch-to-batch phase composition and physical stability studies

			XRD		GVS		
batch	solvent	drying temperature, °C	major phase[a]	minor phase	crystallisation/transition RH, %	phase composition after GVS	TGA weight loss, %
B1	ethyl acetate[b]	70	AM[c]	HH+AHI	55/n.o.	HH	1.8/2.8[d]
B2		60	AM	HH+AHI	55/n.o	HH	7.6
B3		90	AM	AHI	55/n.o	HH	1.2
B4	ethyl acetate abs.	90	AHI	AM	55/40−60	HH	0.3
B5	ethyl acetate abs./ethanol abs. 70/30	70	AHII	n.o.	n.o/93	HH	0.1
B6	ethyl acetate/water 90/10	70	HH	AM	55/93	HH	2.6
B7		70	HH	n.o.	n.o./93	HH	2.8
B8		70	HH	n.o.	n.o./93	HH	2.8

[a] The "major phase" refers to a dominating solid phase present in the sample, while "minor phase" designates other solid phases identified by XRPD. [b] The water activity of the solvent was not controlled. [c] List of abbreviation used for solid-phase identification of ORM10921·HCl: AM - amorphous, AHI - anhydrous phase I, AHII - anhydrous phase II, HH - hemihydrate. [d] TGA analysis was performed also after GVS only for the batch B1.

dx.doi.org/10.1021/op200026f |Org. Process Res. Dev. 2011, 15, 666–672

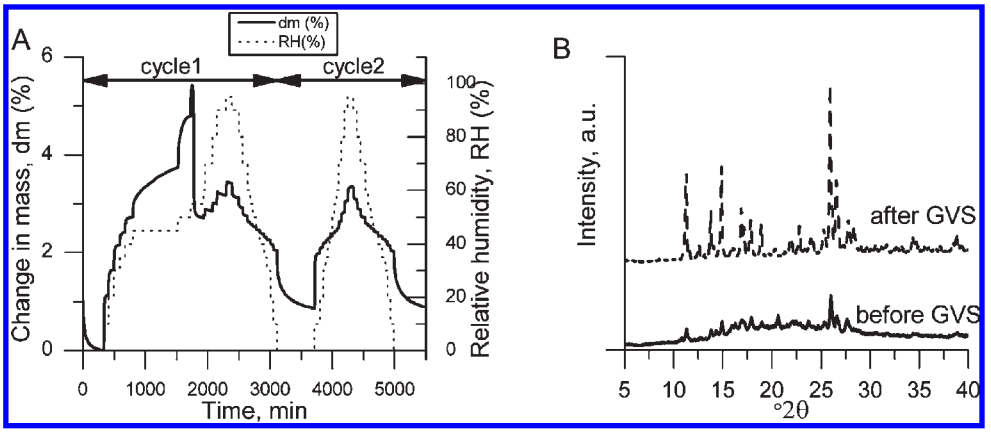

Figure 4. Gravimetrical vapour sorption (GVS) results of the batch B1. (A) Mass change as a function of time and humidity. (B) Humidity-induced solid-phase transformation in the sample revealed by XRPD (analysis performed before and after GVS analysis).

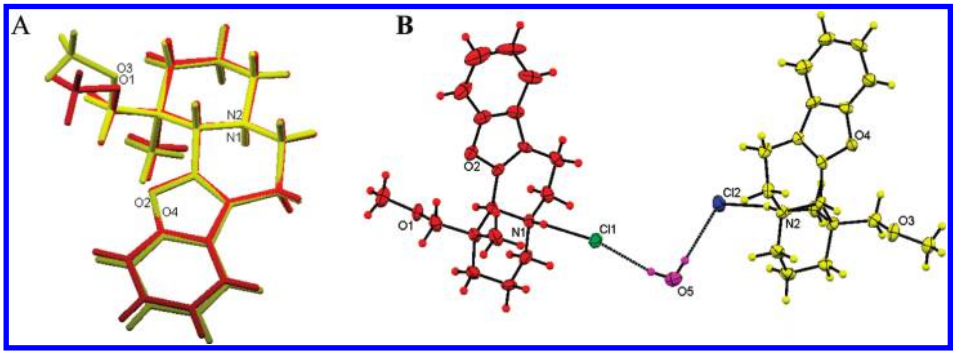

Figure 5. (A) Superimposition of two ORM10921 molecules showing differences in their conformations. (B) Water molecule position in hemihydrate.

observed. First, the TGA weight loss was decreased to 1.2% and, second, AHI (see section 3.3.1) was observed as a minor phase impurity.

The major phase of these batches, however, remained predominantly amorphous, as indicated by amorphous halo and relatively broad peaks on the XRPD patterns (Figure 3). This was also supported by the similarity of the sorption−desorption isotherms of the three batches, B1−B3. The only difference between the isotherms was the maximum amount of moisture uptake (mass change 4.5, 5.5, 8.2% for B1, B2, and B3, respectively) before the crystallization onset at RH = 55%, indicating an increasing amount of amorphous material present in the sample.[23−25] It should be emphasized that the crystallization of amorphous phase in all cases starts at the same RH and appears as a sharp drop of sample mass, which is best illustrated by Figure 4A. This was also the case for the batches B4 and B6, where the amorphous phase was found as a minor one but the major crystalline components were different. The crystallization of amorphous phase in these batches was clearly observed in the GVS mass change curves (not shown). Due to low content of amorphous phase in the batches B4 and B6 the crystallization is not clearly visible in the sorption−desorption isotherms.

The molecule of the ORM10921·HCl (Figure 1) contains quinolizine rings and a freely rotating methoxymethyl group. These structural elements may adopt several more or less stable conformations, giving rise to an intrinsic flexibility of this molecule. Consequently, ORM10921·HCl can exist in multiple solid-state forms due to possible conformational polymorphism,[14,26] which can reduce the crystallization tendency.[26] Indeed, the results of X-ray structure analysis show that the unit cell of the hemihydrate contains two independent ORM10921 molecules, as visualized in Figure 5A. Due to the variation in the relative position of methoxymethyl group, the two molecules adopt different conformations. This provides a possible explanation why our initial attempts to crystallize the salt resulted in predominantly amorphous material. Other reasons can be in the presence of impurities in the batches. The chromatographic purity of the batches has been determined to be between 97.5 and 98.6%.

3.3. Properties of the Discovered Crystalline Forms. *3.3.1. Anhydrous Form AHI.* First, two amorphous batches were found to be contaminated with the hemihydrate form HH (Table 1). This can possibly be attributed to the presence of some amount of water in the crystallization solvent, ethyl acetate, which is known to easily absorb moisture from the atmosphere.[27] To test this hypothesis, the subsequent batch, B4, was crystallized by using dry ethyl acetate and by applying all possible precautions to avoid its contact with the atmospheric moisture. As a result of these adjustments, amorphicity of the batch B4 significantly decreased (Figure 3 and 6B) so that the amorphous phase became the minor one. Moreover, this batch was found to be dominated by a new crystalline form of ORM10921·HCl: AHI (Table 1).

The TGA weight loss of the batch B4 was insignificant (0.3%), leading to the conclusion that the major crystalline phase of these batch is an anhydrate. The DSC traces yielded a single endotherm with an onset at 199 °C (ΔH_f = 65 J/g), which was attributed to the melting of AHI (Figure 7).

dx.doi.org/10.1021/op200026f |*Org. Process Res. Dev.* 2011, 15, 666–672

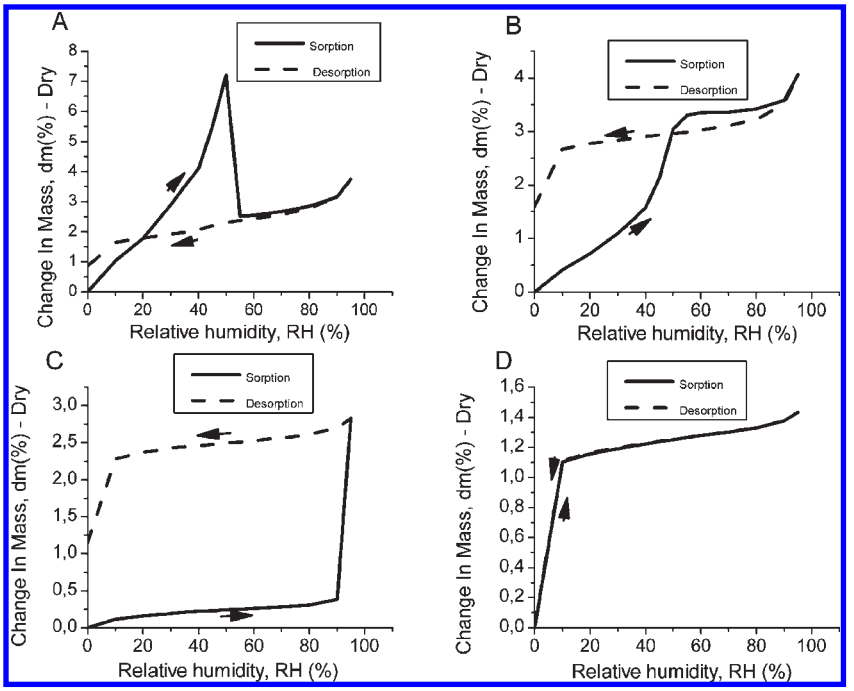

Figure 6. Representative moisture sorption−desorption isotherms of ORM10921·HCl batches studied by gravimetrical vapour sorption (GVS): (A) predominantly amorphous phase AM, (B) anhydrate AHI, (C) anhydrate AHII, (D) hemihydrate HH. Only the first cycle is shown.

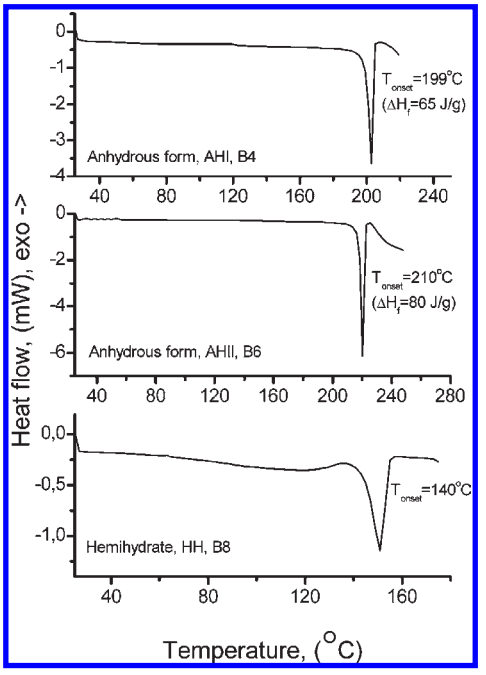

Figure 7. Typical DSC curves of the discovered crystalline solid forms of ORM10921·HCl: anhydrate AHI, anhydrate AHII, and hemihydrate HH.

The distinct phase composition of batches B1−B3 and B4 was also reflected as the differences in their moisture sorption kinetics (Figure 6A,B). At relative humidity lower than 40% the moisture uptake was slower for the batch B4. However, despite its crystalline nature, the new crystalline form AHI was physically unstable, as indicated by the recrystallization taking place at RH = 40−60% and seen as a stepwise jump of the sample mass on the moisture sorption−desorption isotherms. Similar to the case of the predominantly amorphous batches (section 3.2), the resulting crystalline phase was identified as HH (Table 1).

3.3.2. Anhydrous Form AHII. The subsequent batch B5 was crystallized from a mixture of absolute ethyl acetate and absolute ethanol (70:30) as a substitute to absolute ethyl acetate. This slight alteration in the solvent composition caused a profound effect on the crystallization outcome, giving rise to a new solid phase. This single solid phase of batch B5 was identified as another anhydrous (TGA weight loss ~0%, Table 1) crystalline form AHII (Figure 3). Among the previously described forms, AHII was noted to exhibit the highest melting point (T_{onset} = 210 °C) and enthalpy of melting (ΔH_f = 80 J/g) (Figure 7).

AHII was further readily differentiated by a distinctive profile of the moisture sorption isotherm (Figure 6C). As opposed to the earlier batches, it gained almost no moisture (<0.5%) in the range of 0−90% RH, demonstrating relatively high physical stability. However, a sudden weight increment of the sample (about 2.5%) observed at 93% RH was indicative of a phase transformation to a hydrate form. The total amount of water uptake (2.5%) at this point was in a good agreement with the stoichiometry of HH. Thereafter, phase transformation from AHI to HH was verified by XRPD (Table 1).

3.3.3. Hemihydrate HH. The common tendency of all previous batches to undergo a solid-phase transformation to HH suggests a sufficiently high physical stability of this solid form. Hence, the next three batches B6−B8 were designed for direct crystallization of HH (Table 1).

The formation of the desired crystalline form, HH, was verified by comparing the XRPD patterns (Figure 3) and the reference material produced during GVS experiments (section 3.2). The analysis of the XRPD patterns revealed no significant batch-to-batch variations within batches B6−B8, apart from some traces of amorphous material present in batch B6. The conclusion about amorphicity was drawn on the basis of the GVS mass

dx.doi.org/10.1021/op200026f |*Org. Process Res. Dev.* 2011, 15, 666–672

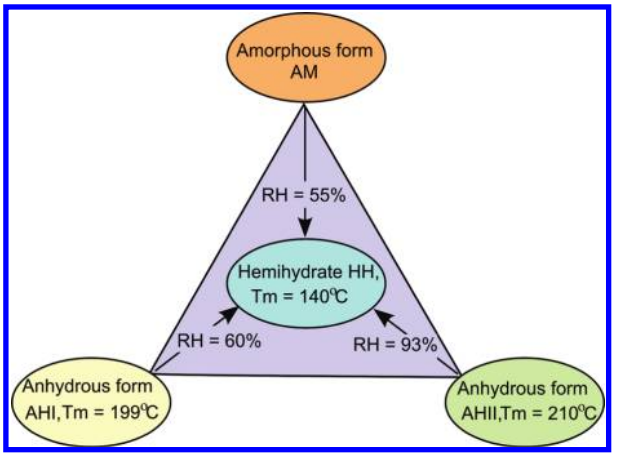

Figure 8. Schematic representation of the relative stability between the discovered solid forms of ORM10921·HCl.

change curve yielding the sharp mass drop at RH = 55% (data not shown).

The results of TGA and DSC analysis for batches B6−B8 also supported the hemihydrate formation. In particular, the TGA weight loss was 2.6−2.8%, corresponding to a half mole of water per one mole of ORM10921·HCl. On the DSC thermogram (Figure 7), the dehydration was seen as a broad endotherm between 90 and 130 °C and was followed by the melting endotherm at 140 °C.

The GVS analysis of batches B6−B8 proved HH to be a relatively stable crystalline material (Figure 6D). First, the sorption and desorption isotherms of these batches were almost identical and exhibited no hysteresis. Second, the hydrate formation/dehydration occurred at RH as low as ≤10%, and thereafter the changes in the sample weight were insignificant (about 0.3%). Finally, it is worth noting that, under the present experimental conditions, the equilibrium water content for HH at 0% RH was approximately 1−1.5%. This was observed most clearly in Figure 4A, where the sample weight change did not drop back to 0% in the beginning of the cycle 2 (RH = 0%). Such behavior of the material indicates that water molecules are tightly bonded by the crystal lattice. This finding was later verified by single-crystal X-ray diffractometry showing that in the HH crystal (Figure 5B) one water molecule binds two different host molecules via H-bond formation with Cl^-, playing role of a binding agent in the structure.

To get better understanding of a hydrate formation potential of ORM10921·HCl, the Cambridge Structure Database (CSD) search was performed for hydrates of HCl salts of organic molecules that contain a tertiary N atom and the only ether's O atoms as H-bond acceptors. This search revealed that in all such structures Cl^- is the only structural element participating in the formation of H-bonds with water. Overall, the Cl^- was found to accept as many as six H-bonds, which is exemplified, for instance, by the crystal structure of VORMEU (CSD refcode). In addition, water molecules are prone to form their own hydrogen-bonding network. Taking into account these two factors, the hydrates with higher numbers of water molecules can be expected. However, only the lowest hydrate form, the hemihydrate (HH), was discovered within this study. Therefore, the structural considerations dictate that a comprehensive polymorph and solvate screening should be performed at the later development phases of the project in order to discover all possible solid-state forms of ORM10921·HCl.

3.4. Stability Relationships among the Discovered Solid Forms of ORM10921·HCl. In order to facilitate the process of solid form selection for early drug development process, the stability relationships among the four discovered solid forms of ORM10921·HCl—amorphous form (AM), anhydrate I (AHI), anhydrate II (AHII), and the hemihydrate (HH)—were deduced by summarizing the results obtained in this study.

Overall, these four solid-state forms can be ranked with respect to their physical stability at ambient conditions in the following order: HH > AHII > AHI > AM. Consequently, due to the superior relative stability of HH, the other three forms demonstrated the propensity to convert into HH under the conditions of high relative humidity, as schematically illustrated in Figure 8. We note, however, that in the presence of hysteresis in the sorption−desorption isotherms the critical water activity cannot be exactly determined from the data, but the data still provide an assessment of the kinetic stability. It should be underlined, however, that the critical RH for crystallization of the amorphous form was extrapolated on the basis of the GVS analyses of the predominantly amorphous batches. The viability of such extrapolation is supported by numerous previous reports, showing that the critical RH for crystallization of amorphous material remains constant irrespective of the amorphous content in the initial material.

Furthermore, when comparing the thermal properties of the two anhydrous forms, AHI (T_{onset} = 199 °C/ΔH_f = 65 J/g) and AHII (T_{onset} = 210 °C/ΔH_f = 80 J/g), the higher melting temperature and melting enthalpy of the form AHII were noted. In accordance with the Burger−Ramberger rule[28] this is an indication of monotropically related polymorphs, with the form AHII being a more stable anhydrous form at all temperatures.

4. CONCLUSIONS

Fast and cost-effective assessment of polymorphism and solvatomorphism tendency and physical stability of the new drug candidate ORM10921·HCl was accomplished. Within this initial study, three crystalline forms, including two anhydrous (AHI and AHII) and one hemihydrate (HH), were discovered. Hence, the polymorphic and pseudopolymorphic tendency of the molecule was ranked as high. Furthermore, the relative stability of the discovered solid forms at ambient conditions was established. The most stable form, the hemihydrate, was selected for future development. The entire project has been completed in three weeks. The procedure reported herein can be also recommended for the evaluation of the polymorphism and solvatomorphism tendency of new chemical entities ("precandidates") even prior to the final selection of a drug candidate.

■ ASSOCIATED CONTENT

Supporting Information. Results of single-crystal analysis of the HH form in *.cif and *.pdf format. This material is available free of charge via the Internet at http://pubs.acs.org.

■ AUTHOR INFORMATION

Corresponding Author

*Telephone: (358) 919159151. Fax: (358) 919159144. E-mail: anna.shevchenko@helsinki.fi.

■ ACKNOWLEDGMENT

Professors Marko Åhlgren and Matti Haukka (Department of Chemistry, University of Eastern Finland) are acknowledged for single-crystal analysis.

■ REFERENCES

(1) Henck, J.-O.; Byrn, S. R. *Drug Discovery Today* **2007**, *12*, 189–199.
(2) Byrn, S. R.; Zografi, G.; Chen, X. *J. Pharm. Sci.* **2010**, *99*, 3665–3675.
(3) Palucki, M.; Higgins, J. D.; Kwong, E.; Templeton, A. C. *J. Med. Chem.* **2010**, *53*, 5897–5905.
(4) Gibson, M. Early Drug Development: Product Design. In *Pharmaceutical Preformulation and Formulation*; Gibson, M., Ed.; Interfarm/CRC: London, New York, WA, 2004.
(5) Huang, L.-F.; Tong, W.-Q. *Adv. Drug Delivery Rev.* **2004**, *56*, 321–334.
(6) Bernstein, J. *Cryst. Growth Des.* **2011**, *11*, 632–650.
(7) Balbach, S.; Korn, C. *Int. J. Pharm.* **2004**, *275*, 1–12.
(8) Byrn, S. R.; Pfeiffer, R. R.; Stowell, J. G. *Solid-State Chemistry of Drugs*; SSCI Inc: West Lafayette, 1999.
(9) Vippagunta, S. R.; Brittain, H. G.; Grant, D. J. W. *Adv. Drug Delivery Rev.* **2001**, *48*, 3–26.
(10) Almarsson, O.; Hickey, M. B.; Peterson, M. L.; Morissette, S. L.; Soukasene, S.; McNulty, C.; Tawa, M.; MacPhee, J. M.; Remenar, J. F. *Cryst. Growth Des.* **2003**, 927–933.
(11) Brittain, H. G. *J. Pharm. Sci.* **2007**, *96*, 705–728.
(12) Hilfiker, R. *Polymorphism in the Pharmaceutical Industry*; Wiley-VCH, Verlag GmbH: Weinheim, 2006.
(13) Descamps, M.; Willart, J. F.; Dudognon, E.; Caron, V. *J. Pharm. Sci.* **2007**, *96*, 1398–1407.
(14) Nangia, A. *Acc. Chem. Res.* **2008**, *41*, 595–604.
(15) Aaltonen, J.; Alleso, M.; Mirza, S.; Koradia, V.; Gordon, K. C.; Rantanen, J. *Eur. J. Pharm. Biopharm.* **2009**, *71*, 23–37.
(16) Brittain, H. G. *Polymorphism in Pharmaceutical Solids*; Marcel Dekker Inc.: New York, 2009.
(17) Gardner, C. R.; Almarsson, O.; Chen, H.; Morissette, S.; Peterson, M.; Zhang, Z.; Wang, S.; Lemmo, A.; Gonzalez-Zugasti, J.; Monagle, J.; Marchionna, J.; Ellis, S.; McNulty, C.; Johnson, A.; Levinson, D.; Cima, M. *Comput. Chem. Eng.* **2004**, *28*, 943–953.
(18) Morissette, S. L.; Almarsson, O.; Peterson, M. L.; Remenar, J. F.; Read, M. J.; Lemmo, A. V.; Ellis, S.; Cima, M. J.; Gardner, C. R. *Adv. Drug Delivery Rev.* **2004**, *56*, 275–300.
(19) Aaltonen, J.; Strachan, C. J.; Poellaenen, K.; Yliruusi, J.; Rantanen, J. *J. Pharm. Biomed. Anal.* **2007**, *44*, 477–483.
(20) Din Belle, D.; Jokela, R.; Tolvanen, A.; Haapalinna, A.; Karjalainen, A.; Sallinen, J. U.S. Patent 7,592,350 B2, 2003.
(21) Berge, S. M.; Bighley, L. D.; Monkhouse, D. C. *J. Pharm. Sci.* **1977**, *66*, 1–19.
(22) Stahl, H. P.; Wermuth, C. G. *Handbook of Pharmaceutical Salts; Properties, Selection, and Use*; Wiley: Weinheim, New York, Chichester, Brisbane, Singapore, Toronto, 2002.
(23) Buckton, G.; Darcy, P. *Int. J. Pharm.* **1995**, *123*, 265–271.
(24) Columbano, A.; Buckton, G.; Wikeley, P. *Int. J. Pharm.* **2002**, *237*, 171–178.
(25) Gorny, M.; Jakobs, M.; Mykhaylova, V.; Urbanetz, N. A. *Drug Dev. Ind. Pharm.* **2007**, *33*, 235–243.
(26) Yu, L.; Reutzel-Edens, S. M.; Mitchell, C. A. *Org. Process Res. Dev.* **2004**, 396–402.
(27) Manek, R. V.; Kolling, W. M. *AAPS PharmSciTech* **2004**, *5* (1), 101−108; DOI 10.1007/BF02830582.
(28) (a) Burger, A.; Ramberger, R. *Mikrochim. Acta* **1979**, *2*, 259–271. (b) Burger, A.; Ramberger, R. *Mikrochim. Acta* **1979**, *2*, 273–316.